International Global Navigation Satellite Systems Association
IGNSS Symposium 2020

Colombo Theatres, Kensington Campus, UNSW Australia
5 – 7 February 2020

UWB Cooperative Localization of Pedestrians along a Constrained Building Hallway

Salil Goel
Department of Civil Engineering, Indian Institute of Technology Kanpur, India
sgoel@iitk.ac.in

Jelena Gabela
Department of Electrical and Electronic Engineering, The University of Melbourne, Australia
jgabela@student.unimelb.edu.au

Guenther Retscher
Department of Geodesy and Geoinformation, Vienna University of Technology, Austria
guenther.retscher@tuwien.ac.at

Charles Toth
Department of Civil, Environmental and Geodetic Engineering, The Ohio State University, USA
toth.2@osu.edu

Andrea Masiero
Interdepartmental Research Center of Geomatics, University of Padova, Italy
masiero@dei.unipd.it

Allison Kealy
Department of Geospatial Science, RMIT University, Australia
allison.kealy@rmit.edu.au

ABSTRACT

In contrast to outdoor localization that relies primarily on GNSS (Global Navigation Satellite Systems) signals, localization in indoor environments is quite challenging due to the absence of GNSS signals and presence of various objects that reflect and disperse the signals such as Wi-Fi (Wireless Fidelity), Ultra-Wide Band (UWB) or other SOP (Signals of Opportunity) used for localization. Cooperative Localization (CL) has proven to be one of the practical approaches for localization in GNSS denied and challenging environments. This paper analyses the experimental performance of an indoor cooperative pedestrian localization approach that relies on UWB based relative range measurements among the pedestrians, as well as relative measurements between the pedestrians and static infrastructure nodes. The experimental setup uses a network containing about 30 static infrastructure nodes and four pedestrians moving in a hallway. Each infrastructure node and pedestrian are equipped with a UWB sensor for relative range measurements. Additionally, some of the pedestrians also carry a low-cost inertial sensor, but inertial observations are not used in this paper. A centralized extended Kalman filter (EKF) is used to localize all the pedestrians using the relative range information and knowledge about the infrastructure nodes. It is observed that

the network geometry perceived by a pedestrian has a significant impact on its localization accuracy. The results demonstrate that the proposed approach can achieve decimetre level localization accuracies, provided a good network geometry, and enough range observations are available. Towards either end of the hallway, significant degradation in the localization accuracy is observed due to the combined effect of the decrease in the number of available range observations and poor network geometry. The accuracy achieved in the proposed setup may be further improved by the inclusion of inertial sensor observations and precise time synchronization among the nodes.

KEYWORDS: Cooperative Localization, Extended Kalman Filter, Indoor Positioning, Ultra-Wide Band

1. INTRODUCTION

Localization in indoor environments can be quite difficult due to the unavailability of GNSS (Global Navigation Satellite Systems) signals. Therefore, various researchers have proposed to use alternate signals such as Wireless Fidelity (Wi-Fi) (Chen and Yang 2003, Bargshady et al. 2010), Ultra-Wide Band (UWB) (Conti et al. 2008, Bargshady et al. 2010, Goel et al. 2017, Goel 2017b, Kealy et al. 2019, Yong et al. 2019) Bluetooth (Faragher and Harle 2015), and other signals (Wymeerch et al. 2009, Shi et al. 2010, Savic and Zazo 2013, Chen et al. 2013, Song et al. 2019). It is quite common to integrate such signals with sensors such as Inertial Measurement Unit (IMU) to derive the 6 DOF (Degrees of Freedom) including 3D position and orientation of pedestrians, manned/unmanned vehicles, etc. Recently, cooperative localization (CL) has demonstrated tremendous potential for positioning in GNSS denied and other challenging environments (Goel 2017b, Pierre Et al. 2018, Yong et al. 2019, Guo et al. 2019). A CL approach incorporates an interconnected network of multiple dynamic (such as pedestrians, unmanned vehicles, etc.) and/or static nodes (called 'anchors') that are capable of measuring relative observations (such as relative range, relative angle, etc.) with respect to the other nodes, and share the information about their own state, as well as, the measured relative information about the other nodes with all (or at least some) nodes in the network (Goel et al. 2016b, Goel et al. 2018a, Pierre et al. 2018, Yong et al. 2019). A CL framework then utilizes this information from all nodes to estimate the state of each node in the network. It is to be noted that, some (or all) of these nodes may be operating in GNSS denied (e.g. indoor) conditions. Even in such conditions, given certain minimum requirements are satisfied, a CL system can be helpful in estimating the states of all nodes, irrespective of the ability of such nodes to receive GNSS signals. The minimum requirements that should be satisfied may include: (a) knowledge of states (and associated covariances) of at least some nodes in a network through some means (through prior knowledge or if some nodes have access to GNSS signals), (b) sufficient connectivity among the nodes (both static and dynamic), (c) and ability of nodes to measure 'appropriate' relative information (depending on the observability conditions) (Goel 2017b, Yong et al. 2019).

A CL system can be classified into either a centralized or a distributed architecture, depending on whether the information is processed centrally or locally by each node. In a centralized architecture, all nodes communicate the information to a central server, that jointly estimates the states of all nodes and communicates it to the respective nodes. In contrast, a distributed or decentralized architecture distributes the processing among all the nodes present in the network, i.e. each node estimates its own state locally and transmits this information to other nodes in the network. A centralized architecture offers better accuracy, while a distributed architecture is scalable, and may offer improved robustness, as distributed network is not prone to 'single point of failure' (Goel 2017b, Goel et al. 2018b). Some of the centralized algorithms proposed

for CL are based on Extended Kalman Filter (EKF) (Goel et al. 2016a, Goel et al. 2016b, Goel et al. 2018a) and Unscented Kalman Filter (UKF). The most commonly used distributed CL algorithms include algorithms based on EKF (Goel 2017a), Belief Propagation (BP) (Wymeersch et al. 2009, Savic and Zazo 2013, Chen et al. 2013), Covariance Intersection Filter (CIF) (Carrillo-Arce et al. 2013), UKF (Shi et al. 2010) and particle filter etc. A cooperative localization system that relies on the presence of a large number of infrastructure/anchor nodes is generally called a P2I (Peer to Infrastructure) based, while an anchor-less network that only makes use of observations between pedestrians/dynamic nodes is called a P2P (Peer to Peer) system (Goel et al 2016b). This paper demonstrates the use of UWB sensor for localization in constrained indoor environments using a centralized cooperative framework. UWB sensors can precisely measure the distance/range between the transmitter and a receiver by measuring two-way time of flight (TW-TOF). Localization in constrained indoor conditions such as long hallways may be even more challenging due to frequent communication loss caused by NLOS (Non-Line-of-Sight) conditions, and poor network geometry that is quite common in such conditions. This paper analyses the performance of UWB based centralized cooperative pedestrian localization system along a constrained building hallway. The tested cooperative system is comprised of about 30 static anchors and four pedestrians. Each anchor is equipped with either a TimeDomain or Pozyx UWB sensor. Similarly, all pedestrians are equipped with either one or both UWB sensors, in addition to inertial sensors and a smartphone that records Wi-Fi observations and camera images. The inertial sensor, Wi-Fi and camera observations are not used in this paper. The anchor nodes can communicate among themselves, as well as, with all pedestrians. Additionally, pedestrians can measure relative ranges among each other. The observations are stored and processed offline using a centralized EKF. The remainder of the paper is organized as follows. Section 2 presents the centralized EKF briefly, and section 3 explains the experimental setup. The results and a discussion are presented in section 4 and conclusions of the paper and recommendations for future work are given in section 5.

2. CENTRALIZED COOPERATIVE EXTENDED KALMAN FILTER

Although various filters such as UKF (Shi et al 2010) have been proposed for centralized CL, EKF is used in this paper due to its relatively lower computational requirements. Furthermore, since the pedestrians are assumed to be moving slowly, and non-linearity in the system is not expected to be very high, EKF is expected to perform suitably well. The cooperative EKF is presented for a general network of *n* pedestrians and *m* anchor nodes, all of which are assumed to be well connected. The connectivity in the network is expected to change as the pedestrians move, due to some nodes being unavailable because of NLOS conditions. The EKF presented here can handle all such cases.

Consider *m* anchor nodes in a cooperative network, whose state is assumed to be known with a given precision. The states of the dynamic pedestrian nodes include 3D position, velocity and acceleration that need to be estimated at every time instant. The joint pedestrian state vector (X_k) includes state of all pedestrian nodes and can be represented by a vector of size $9n\ x\ 1$. Since, the pedestrians are assumed to be moving at slow speed, a constant acceleration model is assumed for pedestrians. The joint state transition matrix (denoted by F_k) for all pedestrians in the network is assumed to be as follows,

$$F_k = \begin{bmatrix} F_k^1 & 0 & . & . & 0 \\ 0 & F_k^2 & . & . & 0 \\ . & . & . & . & . \\ . & . & 0 & F_k^{n-1} & 0 \\ 0 & . & . & 0 & F_k^n \end{bmatrix} \quad (1)$$

This paper assumes that motion of one pedestrian is not directly governed by the motion of other pedestrians and hence, the off-diagonal terms in the above matrix are assumed to be zero. In the above joint matrix, the state transition matrix for the i^{th} pedestrian is denoted as F_k^i and is expressed as follows.

$$F_k^i = \begin{bmatrix} I_{3x3} & I_{3x3}.\delta t & \frac{1}{2}I_{3x3}.\delta t^2 \\ 0_{3x3} & I_{3x3} & I_{3x3}.\delta t \\ 0_{3x3} & 0_{3x3} & I_{3x3} \end{bmatrix} \quad (2)$$

The notations I_{3x3} and 0_{3x3} denote identity and zero matrices, respectively, of size $3x3$. The time increment between two state estimates is denoted by δt. The process noise is assumed to be normally distributed with a zero mean and given covariance matrix Q_k. Each pedestrian can receive at most *m* range observations from anchors, and up to $(n-1)$ range observations from other pedestrians. The joint measurement model for the complete network is represented by equation (3), where $h(.)$ denotes the non-linear measurement model and u_k denotes the measurement noise. This noise is assumed to be normally distributed with zero mean and known covariance R_k. The non-linear measurement model provides a relationship between the pedestrian state and range measurements is denoted by equation (4) (Gabela 2018, Goel 2016a).

$$Z_k = h(X_k) + u_k \quad (3)$$

$$d_k^{i-j} = \sqrt[2]{\left(x_k^i - x_k^j\right)^2 + \left(y_k^i - y_k^j\right)^2 + \left(z_k^i - z_k^j\right)^2} + e_k^{i-j} \quad (4)$$

In equation (4), the notations d_k^{i-j} and e_k^{i-j} denote the distance observation and random range error between nodes i and j at an instant k. The 3D coordinates of the i^{th} node is denoted by $\left(x_k^i, y_k^i, z_k^i\right)$. The joint measurement matrix (denoted by H_k) can be obtained by linearization of equation (3) and is given by equation (5).

$$H_k = \begin{bmatrix} H_k^1 & 0 & 0 & . & 0 \\ 0 & H_k^2 & 0 & . & 0 \\ . & . & . & . & . \\ 0 & 0 & . & H_k^{n-1} & 0 \\ 0 & . & . & 0 & H_k^n \end{bmatrix} \quad (5)$$

In the above equation, the measurement matrix corresponding to the measurements received by the i^{th} node is denoted as H_k^i and is given by equation (6), where $\frac{\partial}{\partial r_k}$ denotes the partial derivative with respect to the position vector (r_k).

$$H_k^i = \begin{bmatrix} \frac{\partial d_k^{i-j}}{\partial r_k} & 0_{1x3} & 0_{1x3} \end{bmatrix} \quad (6)$$

The size of the measurement matrix is dynamic and is governed by the network connectivity, i.e. higher is the connectivity in the network, more will be the number of rows in the measurement matrix. The maximum size of the measurement matrix is achieved when all anchors communicate with all pedestrians and all pedestrians can communicate with all other pedestrians. This maximum size is equal to $[m.n + {}_2^nC]$. It is apparent that as the network size increases, i.e. number of pedestrians increases, the size of measurement matrix and state vector increases, and hence, computational requirements will increase. This is one of the disadvantages of centralized networks. However, centralized systems allow precise computation of correlations among pedestrian states and thus, offer superior localization accuracy compared to distributed systems (Goel 2017b). Since, the complete state space model is now known,

standard EKF equations can be used to perform time updates and measurement updates for the pedestrian states.

3. EXPERIMENTAL SETUP AND DATA AVAILABILITY

To evaluate the experimental performance of the proposed UWB based pedestrian CL, a setup as shown in Figure 1 is used. This experiment is performed at The Ohio State University, USA. All the four pedestrians are moving in a long hallway shown in Figure 1. The UWB anchors are installed on the walls on either side. Some of these anchors are based on TimeDomain UWBs (shown in red), while others are based on Pozyx UWBs (shown in blue). A pedestrian equipped with both UWBs can communicate with either of the anchors, depending on the visibility conditions. According to the manufacturer specifications, TimeDomain range accuracy is about 2-3 cm, while Pozyx range accuracy is of the order of 10 cm. The maximum UWB range achieved in clear outdoor conditions is about 170 m. However, it is expected that range in indoor conditions, especially in hallway type constrained environments, will be considerably less.

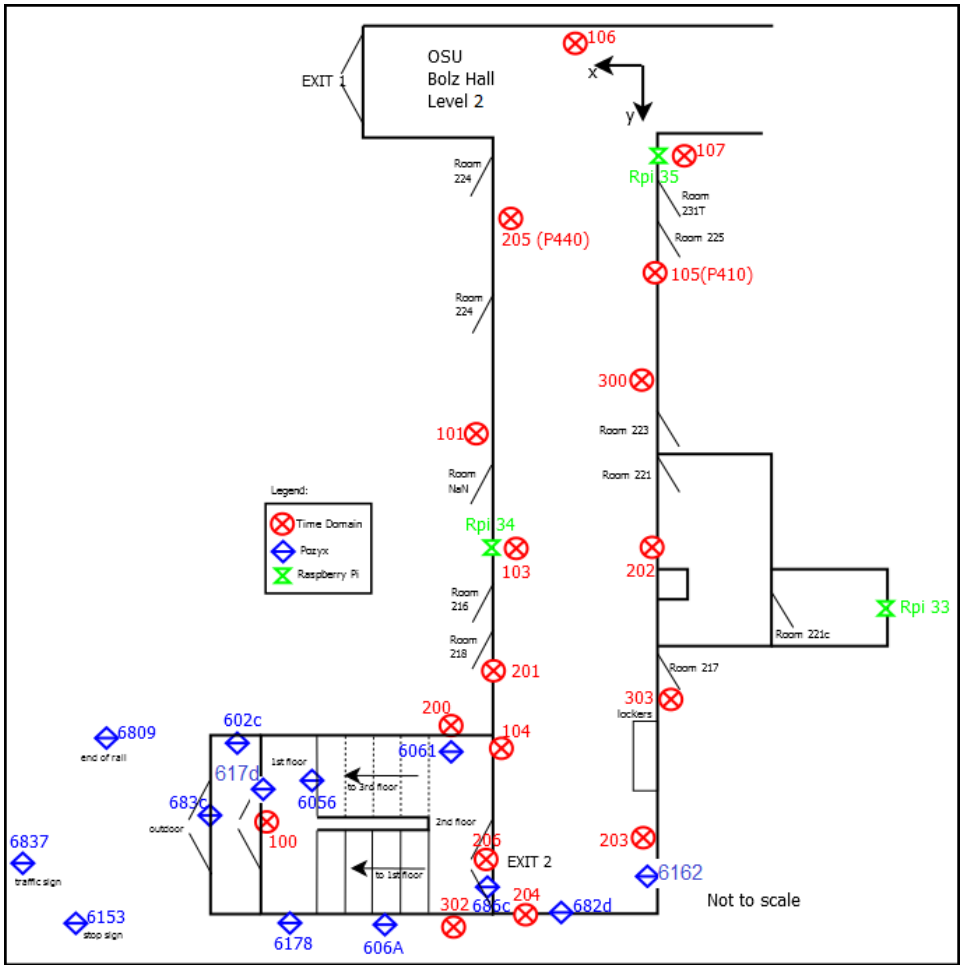

Figure 1: Plan view of the experimental site. The numbers such as 201, 2014, 682d denote the UWB identification tag.

The locations of the anchors are known precisely in a locally defined coordinate system. The anchors locations are determined using a standard surveying procedure. During the data collection activity, no restriction is imposed on the movement of the people in the hallway and therefore, the experimentation is performed in realistic conditions, without imposing any restrictions/constraints. The UWB units on the pedestrians are controlled by a raspberry pi and

are synchronized to the local time. The synchronization is done in an offline mode for all the pedestrians. Since, the pedestrians are moving slowly, high-accuracy synchronization is not required. The total number of UWB observations available to a pedestrian from Pozyx and TimeDomain UWB anchors, as the pedestrian in moving along the hallway, is shown in Figure 2 and Figure 3, respectively. It can be observed that communication of the pedestrian with Pozyx anchors is consistent as compared to TimDomain anchors. Moreover, a larger number of range observations from Pozyx anchors (up to 7) are available for an extended period of time, whereas, sufficient number of TimeDomain range observations are available only at very limited time instants. In the following figures, the notations 'O1', 'S1', etc. indicate the environment (see layout in Figure 1) in which the pedestrian is present at the time it is interacting with UWB nodes. The notations 'O', 'S', and 'I' indicate Outdoor, Staircase and Indoor environments, respectively. For example, a pedestrian starts from an outdoor environment, climbs up the staircase and then transitions into an indoor environment. As seen in Figure 2 and Figure 3, the UWB observations are consistently available in outdoor environments, and suffer from significant outages in staircases and indoor environments.

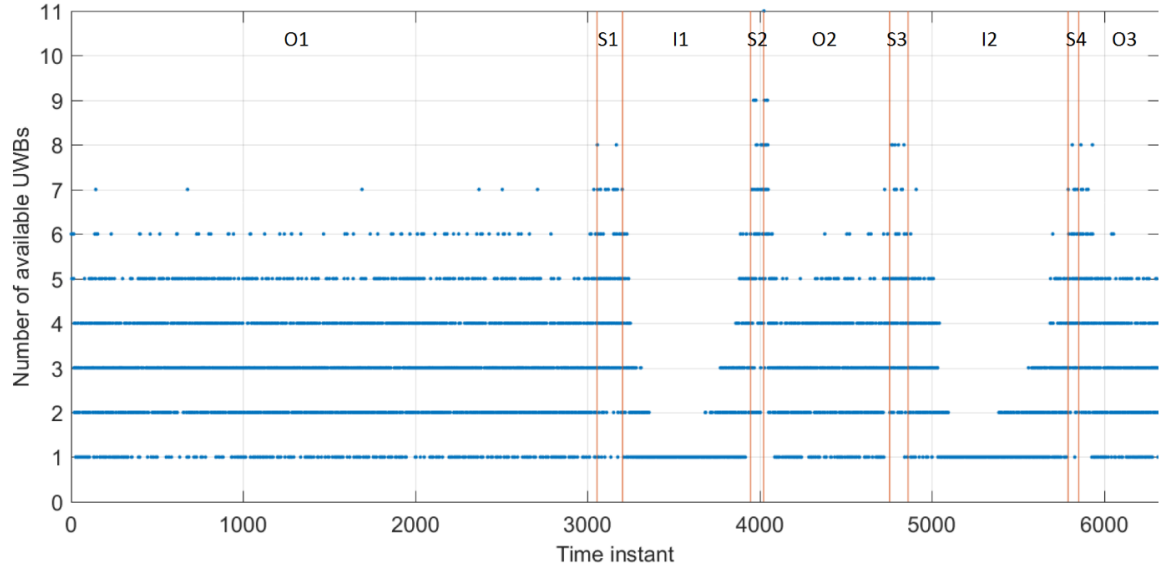

Figure 2: Plot of number of Pozyx UWB observations (with time) available to a pedestrian as the pedestrian is transitioning between different environments such as from outdoor to indoor.

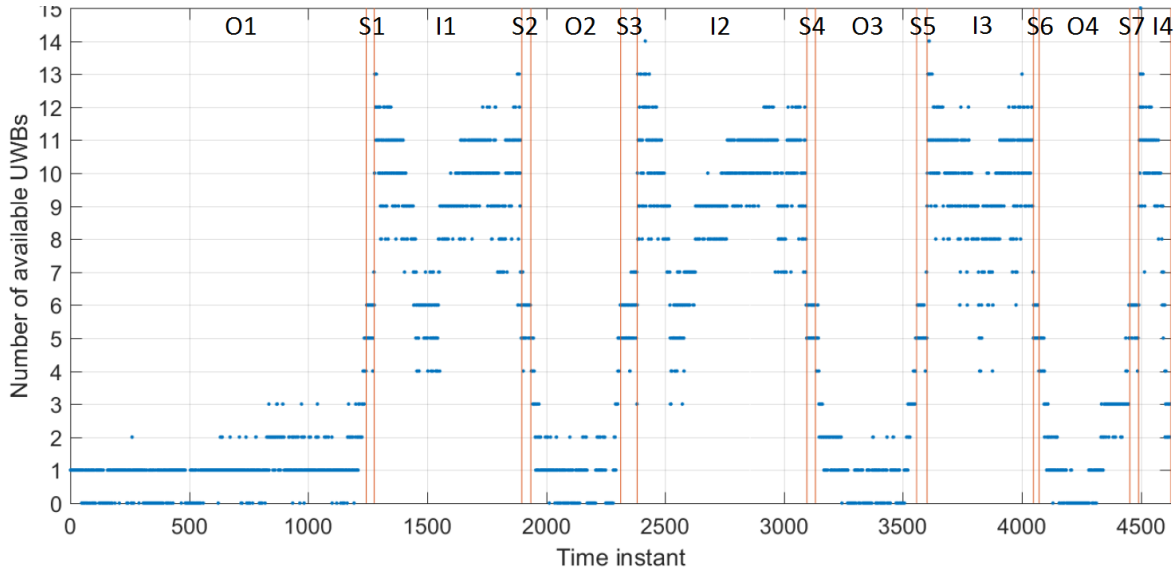

Figure 3: Plot of number of TimeDomain UWB observations (with time) available to a pedestrian as the pedestrian is transitioning between different environments such as from outdoor to indoor.

Communication outages between anchors and pedestrians are expected in indoor and transitional environments due to the restricted LOS. The range measurements to the pedestrians as observed by various anchors is shown in Figure 4, Figure 5 and Figure 6. The communication outages suffered during the pedestrian motion is also visible in these figures.

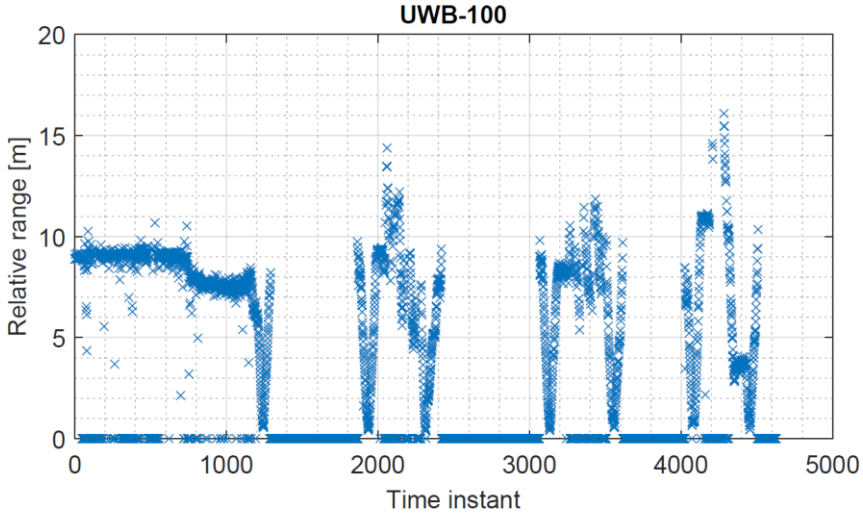

Figure 4: Relative range observations by anchor UWB-100.

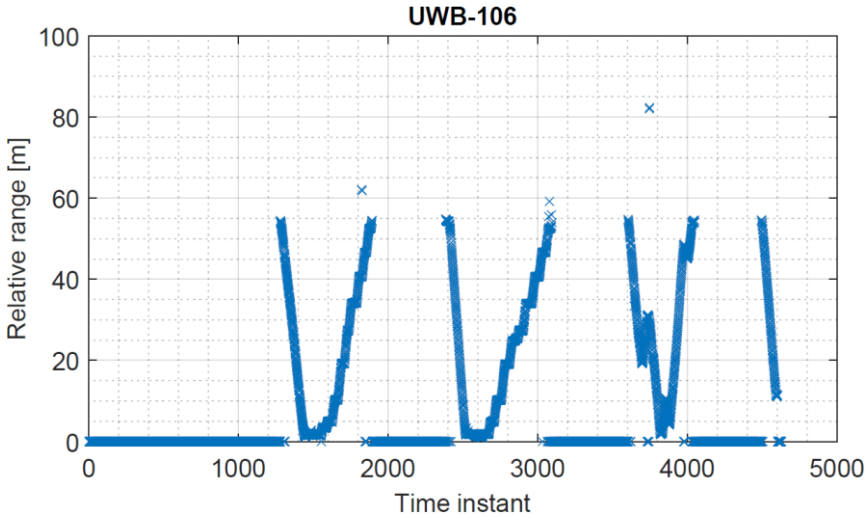

Figure 5: Relative range observations by anchor UWB-106.

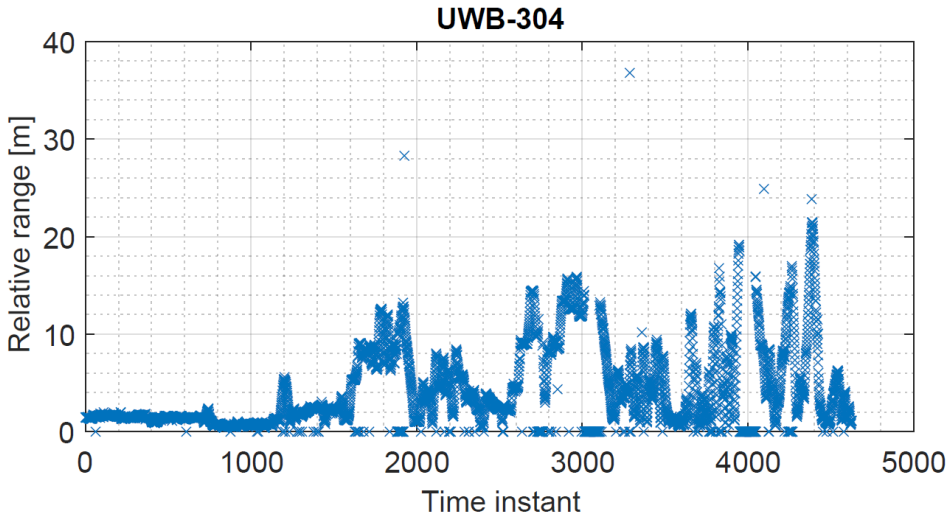

Figure 6: Relative range observations by anchor UWB-304.

It can be seen that ranges of up to 60 m are observed in this setup. Some of the observations are available in outdoor environments, while others are observed indoors. Significant outages between the UWB anchor node and pedestrian are also observed in the three plots shown above. Furthermore, significant outliers in the range observations are also observed at a few instances, especially in indoor environments. Although, some strategies for detection and removal of these outliers have been suggested (for example, see Goel et al. 2018b), this paper does not employ any outlier detection and removal algorithms. It is evident from this section that UWB localization indoor environment can be quite challenging, due to the unavailability of LOS between two pedestrians or between a pedestrian and an anchor. The next section presents the localization results of two of the pedestrians in indoor environments.

4. RESULTS AND DISCUSSION

The time synchronized range observations received by each of the pedestrians is stored and processed offline using the centralized cooperative EKF presented in section 2. To estimate the localization accuracy, fixed checkpoints are used, which were occupied by the pedestrians during the experiment, and the estimated pedestrian location is compared against the checkpoint. The location of the checkpoint is known precisely and estimated using a standard surveying procedure. Since, the indoor environment is flat, only 2D localization accuracy is presented here. Figure 7 and Figure 10 show the colour-coded localization error for two of the pedestrians (C and Z) at the checkpoints. The colour coded HDOP and available UWB observations for pedestrian C is shown in Figure 8 and Figure 9, and for pedestrian Z is shown in Figure 11 and Figure 12.

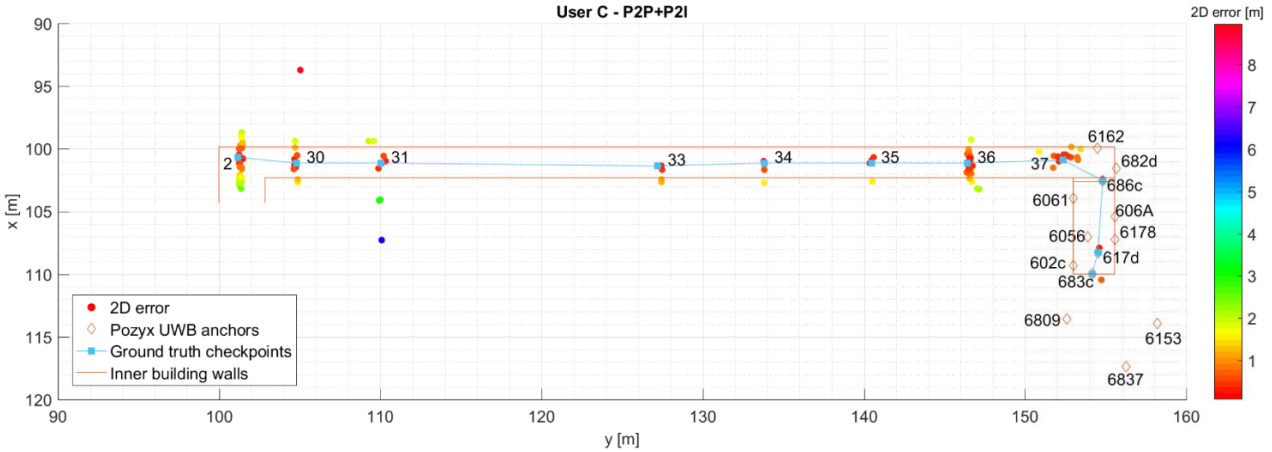

Figure 7: Plot of 2D error for user C in the constrained hallway.

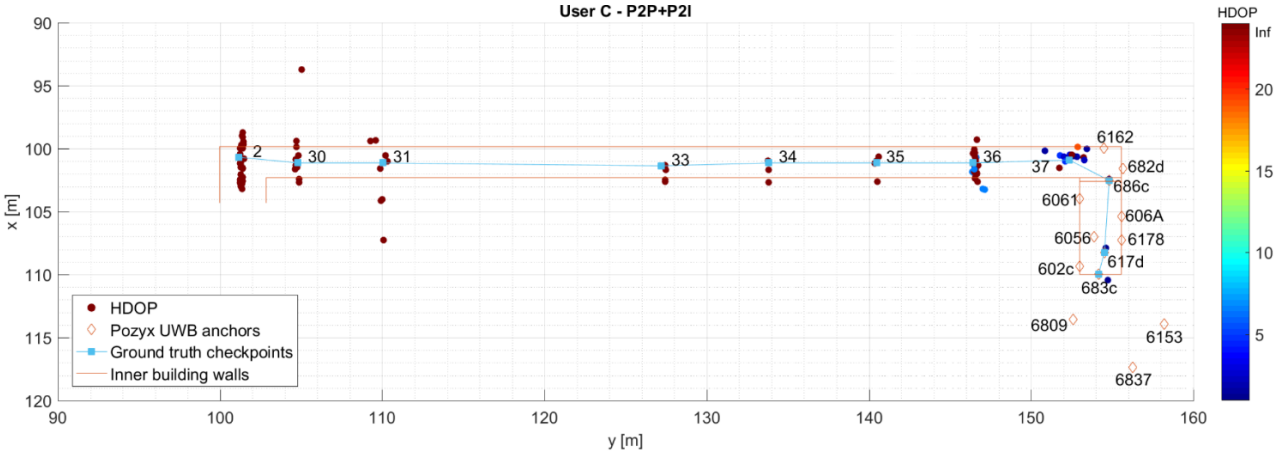

Figure 8: Plot of HDOP for user C in the hallway.

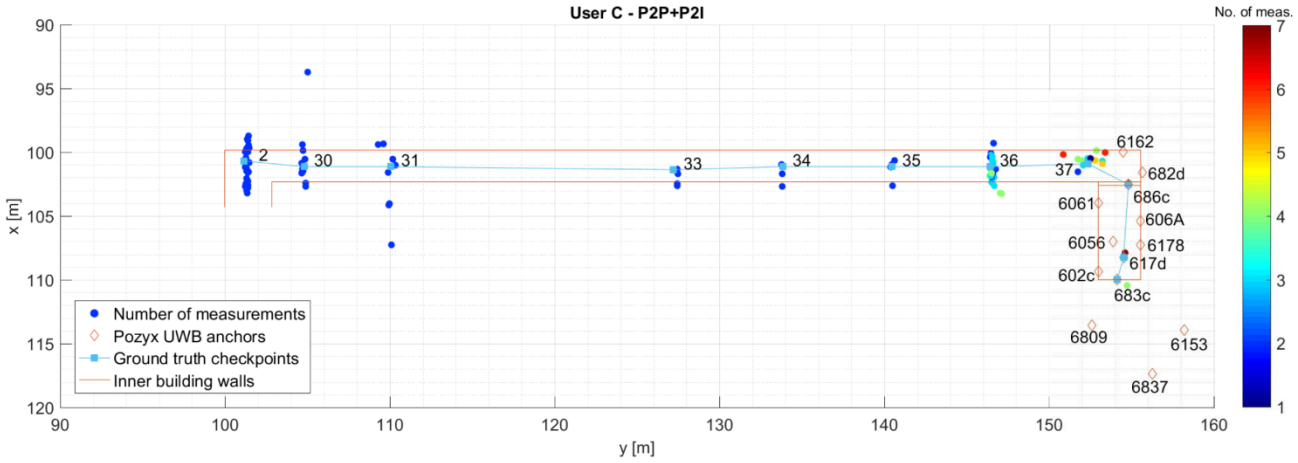

Figure 9: Availability of UWB range measurements to pedestrian C.

To better illustrate the effect of constrained hallway, the map of the hallway is overlaid in these figures. The IDs of the checkpoints are denoted as 2, 30, 31, etc. Since a pedestrian is moving in a stop and go manner, and the pedestrian is stationary for some time on a checkpoint, multiple localization solutions are available at each of the checkpoints. Each dot in Figure 7 to Figure 9 represents an estimated solution. For the user C, it can be observed that the localization accuracy is significantly better in the middle portion of the hallway, as compared to the ends. The localization error at checkpoints 33 to 37 is less than 1 m, while it varies from 2 m to 7 m at checkpoints 2, 30 and 31. The error beyond checkpoint 37 is worse than 5 m. This is most likely due to the unavailability of sufficient number of UWB measurements to the pedestrian, as can be seen in Figure 9. It can be seen only up to 3 range observations are available to the pedestrian C at checkpoints 2, 30 and 31, while the number of range observations vary from 4 to 6 at checkpoints 33 to 37. Beyond checkpoint 37, the range observations are again limited to 3. As would be expected, HDOP value at checkpoints 2, 30 and 31 is very high, and is again due to the unavailability of enough UWB range observations. Despite the unavailability of sufficiently high number of range observations, and presence of outliers in the range data, user C can achieve localization accuracy of a few meters in indoor environments.

The user Z is following user C and can communicate with the anchors installed on the walls, as well as the other pedestrians. The localization solution of user Z is estimated simultaneously along with all pedestrians using the presented centralized framework. Similar to user C, the localization error, HDOP and number of available range observations to user Z is shown in Figure 10, Figure 11 and Figure 12, respectively.

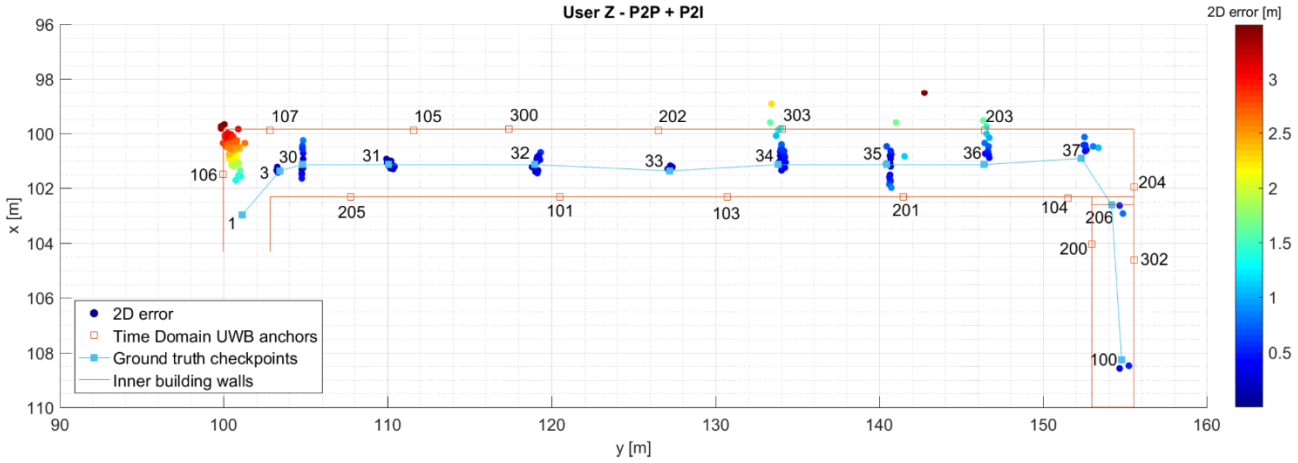

Figure 10: 2D localization error for user Z along the constrained hallway.

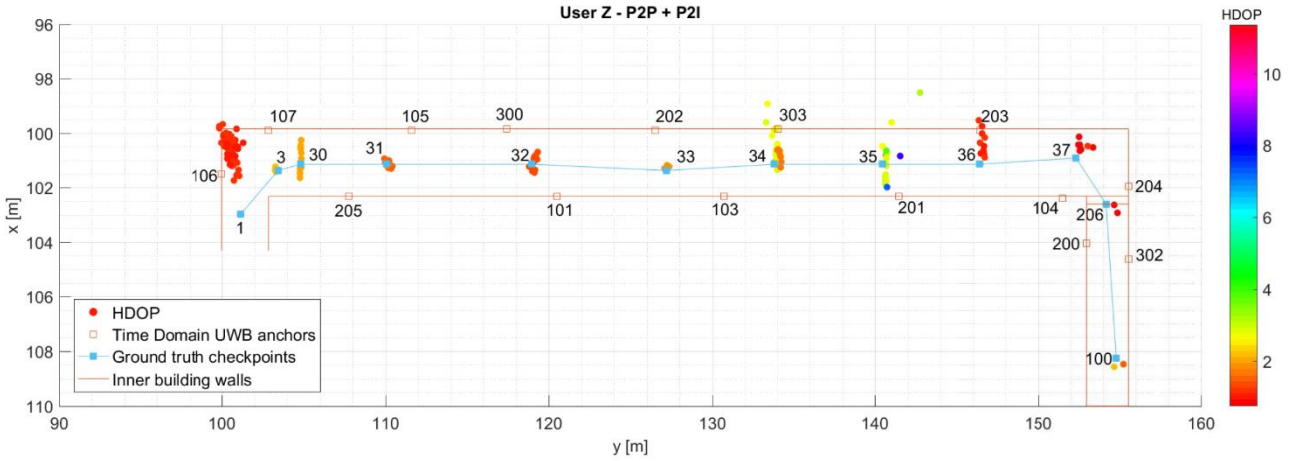

Figure 11: HDOP for user Z along the hallway. HDOP indicates the quality of geometry in the network.

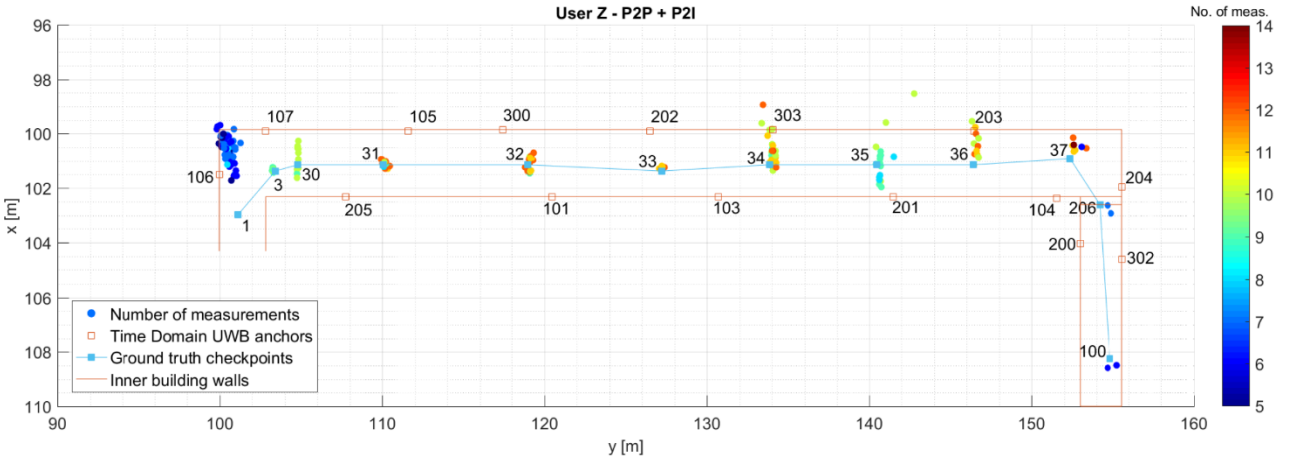

Figure 12: Availability of UWB measurements to user Z as the user is moving along the hallway.

It is interesting to observe that localization error for user Z is of the order of a few meters at the ends of the hallway and is less than 1 m (order of a few decimetre) in the central portion of the hallway. The overall localization accuracy of user Z is much better as compared to user C. One of the reasons for significantly better accuracy of user Z is the presence of sufficiently large number of range observations compared to user C. As can be seen in Figure 12, user Z had access to at least 5 range observations (much higher than user C) during its movement in the hallway. The localization error in the left end of the hallway (near checkpoint 1) is up to 3 m, while at other locations, such as checkpoint 32 – 34, the error is about a few decimetres. Up to 14 range observations are available to user Z at various checkpoints (such as 32 and 33), and thus, localization accuracy at these checkpoints is less than 0.5 m. The HDOP at such locations is significantly lower, which is again favourable to improved accuracy. Compared to the checkpoints 31-33, the localization accuracy at checkpoints 34-36 is a little lower and is most likely due to poor HDOP. Even at the right extreme end of the hallway, i.e. at checkpoint 100, the localization error is up to 1 m, which is significantly better than user C. This is because 5-8 range observations are available to user Z at check point 100, while only up to 3 range observations are available to user C.

These results demonstrate that the proposed setup can achieve decimetre level localization accuracy if a cooperative network is sufficiently well connected and enough range observations (preferable more than 6-7) are available to each of the pedestrians in the network. These range observations could be available from the anchors and/or other pedestrians/dynamic nodes.

Further, experimental results demonstrate that it can be quite challenging for dynamic nodes to receive sufficient range observations needed for localization unless a large number of nodes (either anchors or dynamic nodes) are available in the environment. Even if range observations are available, they may be corrupted or may be susceptible to outliers, and most likely caused by NLOS conditions. Such corrupted observations should be treated appropriately to achieve good quality localization solution in indoor environments.

5. CONCLUSIONS AND FUTURE WORK

This paper presented the experimental performance of a UWB cooperative localization system for pedestrians operating in a constrained building hallway. The developed cooperative system included 4 pedestrians and about 30 anchor nodes. Each pedestrian can measure relative ranges to the other pedestrians, as well as, anchor nodes. The measurements observed in the complete network are processed simultaneously using a centralized architecture to jointly estimate the states of all dynamic nodes in the network. The experimental results demonstrate that achieving a good network connectivity among nodes can be quite challenging in constrained indoor environments. Furthermore, the range observations in such environments may be corrupted by outliers. However, the proposed system can achieve decimetre level accuracy in such constrained environments provided more than 6 range observations are available to each pedestrian consistently. It is found that localization error at the ends of the hallway are significantly poorer (order of a few meters) as compared to the central portion of the hallway. This is due to NLOS conditions at the ends of hallway resulting in fewer range observations available to the pedestrian for localization, coupled with the poor network geometry caused by the elongated shape of the hallway. At the ends of hallway, localization accuracy of the order of 3-6 m has been demonstrated by the system proposed in this paper.

This paper did not utilize the inertial sensors available on the pedestrians. Inclusion of inertial observations such as accelerations and angular rates, may further improve the performance. Further, the accuracy can be improved by imposing restrictions/constraints on the pedestrian movement. For example, a pedestrian cannot run into the walls, and hence, the localization solution should be within the width of the hallway. However, such constraints are not applied in this paper. The future work will include information from the available indoor maps, inertial observations and measurements from other signals such as Wi-Fi and cellular/4G/5G, etc. The accuracy of the developed system can also be improved by inclusion of an adaptive outlier detection algorithm and will be presented in the near future.

ACKNOWLEDGEMENTS

The authors would like to thank Harris Perakis, Vassilis Gikas and Yan Li for assistance during the experimentation and data collection. The support provided by the University of Melbourne to Salil Goel and Jelena Gabela for data collection activities is gratefully acknowledged.

REFERENCES

Bargshady N, Alsindi N. A, Pahlavan K, Ye Y, Akgul F. O (2010) Bounds on performance of hybrid WiFi-UWB cooperative RF localization for robotic applications. *IEEE International Symposium on Personal, Indoor and Mobile Radio Communications*, pp. 277–282, 2010.

Carrillo-Arce L. C, Nerurkar E.D, Gordillo J. L, Roumeliotis, S. I (2013) Decentralized multi-robot cooperative localization using covariance intersection, *IEEE/RSJ International Conference on Intelligent Robots and Systems*, pp. 1412–1417, 2013.

Chen Y, Yang C (2006) A RSSI-based algorithm for indoor localization using ZigBee in wireless sensor network. *Int. J. Digit. Content Technol. its Appl. Digit. Content Technol. its Appl*. 5(7), pp. 407–416, 2006.

Chen X, Gao W, Wang J (2013) Robust all-source positioning of UAVs based on belief propagation. EURASIP, *J. Adv. Signal Process.* 2013(1), pp. 150, 2013.

Conti A., Dardari D, Win M Z (2008) Experimental results on cooperative UWB based positioning systems. *Proc. IEEE ICUWB*, vol.1. Hanover, Germany, pp. 191–195, 2008.

Faragher F, Harle R (2015) Location Fingerprinting with Bluetooth Low Energy Beacons. *IEEE Journal on Selected Areas in Communication* 33(11), pp. 2418-2428, 2015.

Gabela J, Goel S, Kealy A, Hedley M, Williams S (2018) Cramer Rao Bound Analysis for Cooperative Positioning in Intelligent Transportation Systems, *Proceedings of International Global Navigation Satellite Systems (IGNSS) Symposium 2018*, Sydney, Australia, February 7-9, 2018, Available at: http://www.ignss2018.unsw.edu.au/sites/ignss2018/files/u80/Papers/IGNSS2018_paper_21.pdf (Accessed November 11, 2019).

Goel S, Kealy A, Lohani B (2016a) Cooperative UAS localization using low cost sensors, *ISPRS Annals of Photogrammetry Remote Sensing and Spatial Information Sciences* III-1: 183-190, doi:10.5194/isprs-annals-III-1-183-2016.

Goel S, Kealy A, Lohani B (2016b) Infrastructure vs Peer to Peer Cooperative Positioning: A comparative analysis, *Proceedings of ION GNSS+ 2016*, Portland, Oregon, USA, September 12-16, 2016.

Goel S (2017a) A Distributed Cooperative UAV Swarm Localization System: Development and Analysis, *Proceedings of the 30th International Technical Meeting of The Satellite Division of the Institute of Navigation (ION GNSS+ 2017)*, Portland, Oregon, September 25-29, 2017, pp. 2501-2518.

Goel S, (2017b) Cooperative Localisation of Unmanned Aerial Vehicles using Low-Cost Sensors, *PhD Thesis*, Department of Infrastructure Engineering, The University of Melbourne, Melbourne, Australia.

Goel S, Kealy A, Gikas V, Retscher G, Toth C, Brzezinska DG, Lohani B (2017) Cooperative Localization of Unmanned Aerial Vehicles Using GNSS, MEMS Inertial and UWB Sensors, *Journal of Surveying Engineering* 143(4), DOI:10.1061/(ASCE)SU.1943-5428.0000230.

Goel S, Kealy A, Lohani B (2018a) Posterior Cramer Rao Bounds for Cooperative Localization in Low-Cost UAV Swarms, *Journal of the Indian Society of Remote Sensing*, 47(4), DOI: 10.1007/s12524-018-0899-3

Goel S, Kealy A, Lohani B (2018b) Development and Experimental Evaluation of Low-Cost Cooperative UAV Localization Network Prototype, *Journal of Sensor and Actuator Networks*, 7(4), DOI: 10.3390/jsan7040042

Guo K, Li X, Xie L (2019) Ultra-Wideband and Odometry-Based Cooperative Relative Localization with Application to Multi-UAV Formation Control, *IEEE Transactions on Cybernetics*, DOI: 10.1109/TCYB.2019.2905570

Kealy A, Retscher G, Gabela J, Li Y, Goel, S, Toth, C, Masiero A, Blaszczak-Bak W, Gikas V, Perakis, H, Koppanyi Z, Grejner-Brzezinska, D (2019) A Benchmarking Measurement Campaign in GNSS-denied/Challenged Indoor/Outdoor and Transitional Environments, *FIG Working Week*

2019: Geospatial Information for a Smarter Life and Environmental Resilience, Vietnam, April 22-26, 2019.

Penna F, Caceres M. A, Wymeersch H (2010) Cramér-Rao Bound for Hybrid GNSS Terrestrial Cooperative Positioning. *IEEE Commun. Lett.*, 14(11), pp. 1005–1007, 2010.

Pierre C, Chapuis R, Aufrere R, Laneurit J, Debain C (2018) Range-only based Cooperative Localization for Mobile Robots, *Proc. 21st International Conference on Information Fusion*, pp. 1933-1939.

Savic V, Zazo S (2013) Cooperative localization in mobile networks using nonparametric variants of belief propagation. *Ad Hoc Networks* 11(1), pp. 138–150, Jan. 2013.

Shi X, Wang T, Huang B, Zhao C (2010) Cooperative multi-robot localization based on distributed UKF. *Proc. - 2010 3rd IEEE Int. Conf. Comput. Sci. Inf. Technol. ICCSIT 2010*, vol. 6, pp. 590–593, 2010.

Song Y, Guan M, Peng Tay W, Look Law C, Wen C (2019) UWB/LiDAR Fusion for Cooperative Range-only SLAM. *Proc. IEEE International Conference on Robotics and Automation*, Montreal, Canada, May 20-24, 2019, pp. 6568-6574,

Wymeersch H, Lien J, Win M. Z (2009) Cooperative localization in wireless networks, *Proc. IEEE* 7(2), pp. 427–450, Feb. 2009.

Yong G, Cai Z, Dong H (2019) A High Precision Indoor Cooperative Localization Scheme Based on UWB Signals, In: *Jia M., Guo Q., Meng W. (eds) Wireless and Satellite Systems. WiSATS 2019*. Lecture Notes of the Institute for Computer Sciences, Social Informatics and Telecommunications Engineering, vol 281. Springer, Cham, DOI: 10.1007/978-3-030-19156-6_59